Nucleon Transfer in $^{10}B(^{14}N,^{13}N)^{11}B$, $^{10}B(^{14}N,^{11}C)^{13}C$, and $^{40}Ca(^{14}N,^{13}N)^{41}Ca$ Reactions*†

J. G. COUCH‡ AND J. A. MCINTYRE§
Texas A&M University, College Station, Texas

AND

J. C. HIEBERT‖
Oak Ridge National Laboratory, Oak Ridge, Tennesee

(Received 29 July 1966)

Thin targets of ^{10}B and ^{40}Ca were bombarded with ^{14}N ions from the Oak Ridge tandem van de Graaff accelerator. Ranges, angular distributions $d\sigma(\theta)/d\Omega$, and total cross sections $\sigma(E)$ were obtained by measuring the activities of the positron emitters ^{13}N and ^{11}C formed in the neutron and proton transfer reactions. The $^{10}B(^{14}N,^{13}N)^{11}B$ reaction was shown to involve primarily ground states of ^{11}B at an incident energy of 16.3 MeV. The angular-distribution data for this reaction were found, in their dependence on angle, to be consistent with tunneling-theory calculations. [Although cross-section calculations with the tunneling theory have been limited to the $^{14}N(^{14}N,^{13}N)^{15}N$ reaction, the angular dependence calculated for the differential cross section can be used for other reactions.] A reduced width for the transferred neutron could not be determined, however, because of the specialization of the calculations to the $^{14}N(^{14}N,^{13}N)^{15}N$ reaction. In the $^{10}B(^{14}N,^{11}C)^{13}C$ reaction, the protons transfer to both the ground state and first excited state of ^{13}C, but no transfers involving the first excited state of ^{11}C were observed. For the $^{40}Ca(^{14}N,^{13}N)^{41}Ca$ experiments, reactions were found at the higher energies measured (>27.5 MeV) which led to excited states as well as to the ground state of ^{41}Ca. Again, the angular distributions were found to be consistent with the tunneling process. Total-cross-section data were also obtained which can be used for a neutron reduced-width determination in ^{41}Ca when the theory has been extended to this reaction (with the reservation that there is no evidence available that only one state in ^{41}Ca is involved in the transfer-process energies below 27.5 MeV).

I. INTRODUCTION

In view of recent successes[1–3] in extracting reduced widths from the $^{14}N(^{14}N,^{13}N)^{15}N$ reaction, two additional reactions involving neutron transfer have been investigated experimentally in the hope that the theories can be extended to apply to them also. In this earlier work, the semiclassical tunneling (SCT)[4–7] and distorted-wave Born-approximation (DWBA)[2] theories had been found to be in good agreement with the data[1,8] of the $^{14}N(^{14}N,^{13}N)^{15}N$ reaction at energies well below the Coulomb barrier. At higher energies the agreement was spoiled by the onset of nuclear absorption presumed to occur within some critical distance of closest approach, as evidenced by angular-distribution data.

The $^{10}B(^{14}N,^{13}N)^{11}B$ reaction has been chosen for the present study primarily because of its similarities to the $^{14}N(^{14}N,^{13}N)^{15}N$ reaction. In both of these cases the reaction involves light nuclei of similar mass, and the neutron transfers between $1p$ shells. The boron reaction differs, however, since the interacting particles are not identical, and a $p_{3/2}$ rather than $p_{1/2}$ neutron state is involved in the residual nucleus. A further motivation for the work is that a reduced-width value for ^{11}B has been reported[3] recently, where the SCT theory was applied to total-cross-section data of the $^{10}B(^{14}N,^{13}N)^{11}B$ reaction at energies presumably below the Coulomb barrier. There has as yet been no investigation of nuclear-absorption effects at these energies. In addition, previous range studies[9] had been done only at energies above the Coulomb barrier where it was found that, although some ground-state tunneling occurred at 28.0 MeV at the forward angles, none occurred at 19.8 MeV. It was therefore necessary for Gaedke *et al.*[3] to assume absorption effects to be small and ground-state transfers to be predominant at their energies (9.5–11.5 MeV); these assumptions are based indirectly on the results of the $^{14}N(^{14}N,^{13}N)^{15}N$ studies.[1,8] In the present investiga-

* Research sponsored in part by the U. S. Atomic Energy Commission under contract with the Union Carbide Corporation.

† Material supplementary to this article has been deposited as Document No. 9116 with the ADI Auxiliary Publications Project, Photoduplication Service, Library of Congress, Washington, D. C. 20540. A copy may be secured by citing the document number and by remitting $1.25 for photoprints, or $1.25 for 35-mm microfilm. Advance payment is required. Make checks or money orders payable to: Chief, Photoduplication Service, Library of Congress.

‡ Oak Ridge Graduate Fellow from Texas A&M University under appointment from the Oak Ridge Associated Universities. Present address: Physics Department, Washington State University, Pullman, Washington.

§ Partially supported by an Oak Ridge Associated Universities research participation contract.

‖ U. S. Atomic Energy Commission Postdoctoral Fellow under appointment from the Oak Ridge Associated Universities, 1963–1965. Present address: Physics Department, Texas A&M University, College Station, Texas.

[1] L. C. Becker and J. A. McIntyre, Phys. Rev. **138**, B339 (1965).

[2] P. J. A. Buttle and L. J. B. Goldfarb, Nucl. Phys. **78**, 409 (1966).

[3] R. M. Gaedke, K. S. Toth, and I. R. Williams, Phys. Rev. **141**, 996 (1966).

[4] G. Breit and M. E. Ebel, Phys. Rev. **104**, 1030 (1956).

[5] G. Breit, in *Handbuch der Physik*, edited by S. Flügge (Springer-Verlag, Berlin, 1959), Vol. 41, Part 1.

[6] G. Breit, K. W. Chun, and H. G. Wahsweiler, Phys. Rev. **133**, B403 (1964).

[7] G. Breit, Phys. Rev. **135**, B1323 (1964).

[8] J. C. Hiebert, J. A. McIntyre, and J. G. Couch, Phys. Rev. **138**, B346 (1965).

[9] K. S. Toth, Phys. Rev. **131**, 379 (1963).

tion, ranges and angular distributions as well as total cross sections are measured for the $^{10}B(^{14}N,^{13}N)^{11}B$ reaction in an effort (1) to determine the ground-state contribution to the neutron transfer process, and (2) to determine the effects of nuclear absorption on the transfer process. The proton transfer reaction $^{10}B(^{14}N,^{11}C)^{13}C$ was also studied since the data were collected along with those obtained for the neutron transfer reaction.

The $^{40}Ca(^{14}N,^{13}N)^{41}Ca$ reaction was also studied. This reaction differs from the above reactions in that the neutron transfers to an f shell in forming the ground state of ^{41}Ca. No previous data are available for this reaction.

A comment is appropriate concerning the use made of the tunneling theories in this paper. Only two calculations, the SCT[4–7] and the DWBA,[2] have been published which are complete enough to permit the determination of the reduced widths associated with the transferred neutron. Both of these calculations have been specialized, however, to the $^{14}N(^{14}N,^{13}N)^{15}N$ reaction and cannot be used, therefore, to determine reduced-width values in reactions involving different neutron angular-momentum quantum numbers. However, Buttle and Goldfarb[2] have noted that angular distributions should be relatively independent of the quantum numbers of the transferred neutron, so that the tunneling calculations for the $^{14}N(^{14}N,^{13}N)^{15}N$ reaction properly modified for boron and calcium parameters have been used in this paper to assist in evaluating the experimental angular-distribution data. The total-cross-section data, however, cannot be evaluated with the tunneling theories as presently developed. Nevertheless, for orientation purposes only, the SCT tunneling theory has been plotted in Figs. 9 and 10 along with the total-cross-section experimental data.

II. EXPERIMENTAL PROCEDURE

The scattering chamber and detection system used here have been described before.[10,11] Briefly, the scattering chamber provides for the collection of the reaction products (in this case ^{13}N and ^{11}C) on plastic tapes or in stacks of thin foils for measuring angular distributions or range distributions. Measurement of the radioactivity of the foils or tapes was done with a detection system which included a shielded complex of 20 coincidence counters with NaI detectors. The data were stored in the memory of a multichannel analyzer.[8]

The ^{14}N beams were supplied by the Oak Ridge tandem van de Graaff accelerator. The absolute value of the beam energy was known to ± 100 keV, and the beam-energy resolution was 10 keV.

The range measurements of the outgoing ^{13}N and ^{11}C nuclei were made with stacks of plastic[12] and nickel[13] foils about 400 $\mu g/cm^2$ thick. The range-energy data of Northcliffe[14] were used to convert the ranges to energies. For the ^{10}B experiments, good range data could be obtained since the reaction-product nuclei leave the target at small angles and a "transmission" geometry can be used for the target. At the large angles studied in the ^{40}Ca experiments, however, the reaction products left the target from the same face as the entering beam particles. The total path length of the incoming beam particle and outgoing reaction particle thus varied from zero for reactions at the target beam-entrance surface to a maximum at the beam-exit surface. This effect degraded the energy resolution of the foil stack for the large-angle measurements.

Total-cross-section measurements were made with the thin target mounted in the beam-collecting Faraday cup. A collector foil in the forward direction collected all reaction products in the ^{10}B experiments. For the ^{40}Ca, where the ^{13}N emerged in the back direction, a cylindrical foil, axially aligned with the beam, collected particles emerging at all but the largest angles. The angular-distribution data were used to correct for the particles missed by this collector.

The reaction products collected were identified through their decay half-lives. Since the detection system[11] was sensitive only to positron emitters, only the nuclei ^{15}O(2.1 min), ^{13}N(10.0 min), and ^{11}C(20.5 min) were detected. A least-squares fit computer program[15,16] was used to determine the contributions of the different nuclei to the radioactivity observed.

III. RESULTS

A. Ranges

Measurements of the terminal ranges of ^{11}C and ^{13}N from the $^{14}N+^{10}B$ reactions were taken at 15°, 20°, 30°, 40°, and 50° at 16.3-MeV lab energy (Fig. 1), and 30° at 19.8-MeV lab energy (Fig. 2). The data points of each curve represent the relative amounts of activity measured in the layers of nickel foils, and the error bars represent the counting errors. The various data curves have been corrected for background and normalized to within an estimated 30% error. Smooth curves have been drawn through the data points to identify the peak locations and widths. These peaks show a typical range spread at half-maximum of four foils, or about 1.6 MeV.

The energy diagrams above the curves in Figs. 1 and 2

[10] J. A. McIntyre, T. L. Watts, and F. C. Jobes, Nucl. Instr. Methods 21, 281 (1963).
[11] F. C. Jobes, J. A. McIntyre, and L. C. Becker, Nucl. Instr. Methods 21, 304 (1963).
[12] T. L. Watts and C. J. Sneider, Nucl. Instr. Methods 21, 296 (1963).
[13] Supplied by Chromium Corporation, Waterbury, Connecticut.
[14] L. C. Northcliffe, Ann. Rev. Nucl. Sci. 13, 67 (1963); Natl. Acad. Sci.—Natl. Res. Council, Publ. 1133 (1964); privately distributed curves.
[15] We are indebted to Dr. T. L. Watts for the computer program which is similar to the FRANTIC [P. C. Rogers, MIT Laboratory of Nuclear Science, Technical Report No. 76, 1962 (unpublished)].
[16] The least-squares procedure used here follows closely the analysis described in W. C. Hamilton, *Statistics in Physical Science* (Ronald Press Company, New York, 1964).

predict the depths of penetration of the ^{13}N and ^{11}C particles from ground-state and first-excited-state reactions; the error in predicting these peak locations is estimated to be less than two foil layers based upon an estimated 5% error in range values.[14]

The peaks in Figs. 1 and 2 are designated by either ^{11}C or ^{13}N, depending on the half-life of the activity collected in the foils. These half-lives were determined from a least-squares analysis of the common decay curve obtained by combining the activities of several foil layers in each peak and are pure to within 10%. This analysis could not be done for the foils individually because of the very low activities involved.

The 19.8-MeV data of Fig. 2 show that ^{13}N from transfers to the ground state of ^{11}B scatter at 30°, but none scatter at that angle from excited states of ^{11}B. The

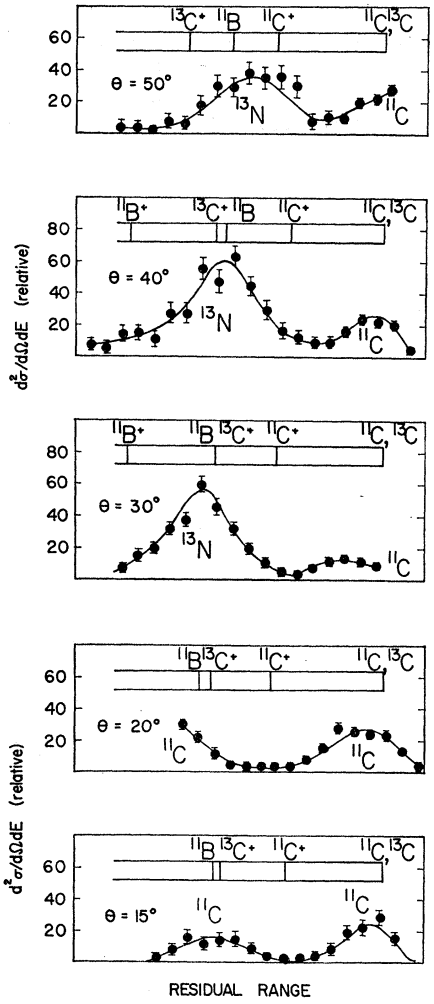

FIG. 1. Range distributions of ^{13}N and ^{11}C from ^{14}N+^{10}B reactions at 16.3 MeV. Each datum point represents one foil layer, and the energy diagram predicts the peak locations (±2 foils). Each peak is labeled ^{11}C or ^{13}N, based on the half-life of foil activity. The ordinate scale is the same for all sets of data. The angles are measured in the lab system.

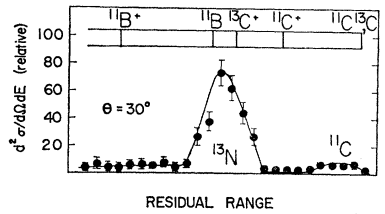

FIG. 2. Range distributions of ^{13}N and ^{11}C from ^{14}N+^{10}B reactions at 19.8 MeV. Each datum point represents one foil layer, and the energy diagram predicts the peak locations (±2 foils). Each peak is labeled ^{11}C or ^{13}N, based on the half-life of foil activity. The angle is measured in the lab system.

data also show some ^{11}C from reactions in which both ^{11}C and ^{13}C were formed in the ground state, but reactions where ^{11}C were left in the first excited state are noticeably absent. Few, if any, reactions occur at this angle where the ^{13}C are formed in the first excited state, as evidenced by the lack (see above remarks) of 20.5-min activity in the large center peak. In contrast, Toth[9] found no ^{13}N involving ground states at this energy. There also was no indication in his work of ^{11}C at this angle where only ground states of ^{11}C and ^{13}C were formed, but his data showed that reactions involving the first excited state of either ^{11}C or ^{13}C probably did occur.

The terminal ranges of ^{13}N in the foil stacks from the ^{14}N+^{40}Ca reaction are shown in Fig. 3, which includes data taken at lab angles of 70°, 80°, and 90° at 29.8-MeV, and 90° at 27.5-MeV lab energy. These data were analyzed in the same manner as the ^{14}N+^{10}B ranges above, except that only ^{13}N were detected in the foils. In the energy diagram of Fig. 3, the right and left vertical lines represent, respectively, the ^{41}Ca ground-state and first-excited-state peak locations.

B. Angular Distributions

Angular distributions of ^{11}C and ^{13}N were determined at five energies, the data being displayed in Figs. 4 and

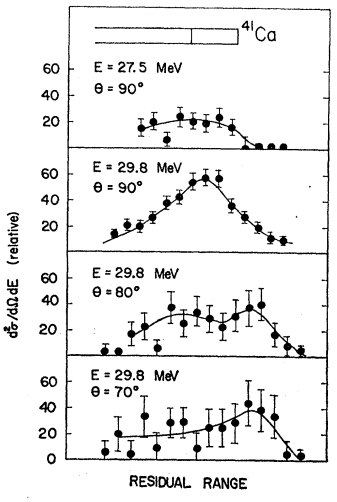

FIG. 3. Range distributions of ^{13}N from ^{40}Ca(^{14}N,^{13}N)^{41}Ca at 27.5 and 29.8 MeV. Each datum point represents one layer of foils. The energy diagram shows the predicted peak locations (±2 foil layers) of ^{13}N from ground-state and first-excited-state transfers.

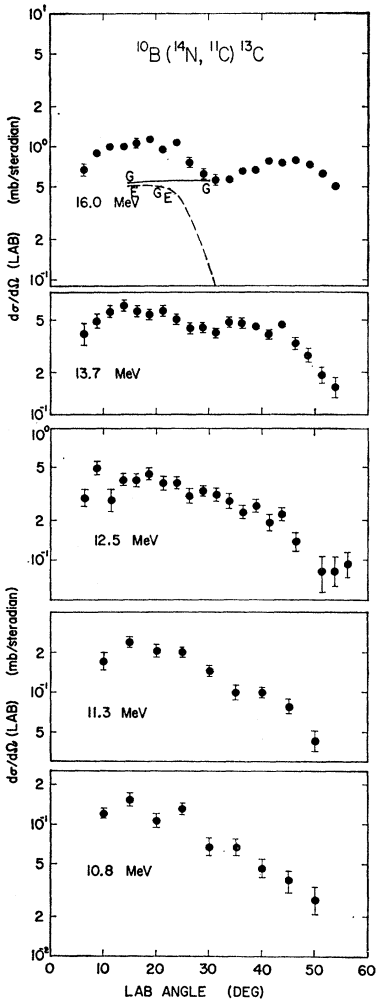

FIG. 4. Angular distribution of ^{11}C from $^{10}B(^{14}N,^{11}C)^{13}C$. At 16.0 MeV, the small-angle peak is separated into ground-state (solid curve) and excited-state (dashed curve) contributions, as determined from range-distribution measurements. The large-angle peak is due to ground-state transfers only.

5. Absolute differential-cross-section values were obtained at each energy by integrating the ^{11}C (relative) angular distributions over all lab angles and comparing the sum to the measured total-cross-section value for $^{10}B(^{14}N,^{11}C)^{13}C$ at that energy. The same factors used to normalize the ^{11}C data at each energy were also used to normalize the ^{13}N relative-angular-distribution curves to an absolute scale, because the ^{13}N and ^{11}C distributions were collected simultaneously at each energy. Although extrapolations were necessary in carrying out the above integrations, it is estimated that these absolute normalizations are accurate to within 20%. The data at each energy represent an average of at least two independent measurements. The error bar associated with each datum point of Figs. 4 and 5 includes only the standard error from the least-squares half-life analysis.

Angular distributions of ^{13}N from $^{13}N+^{40}Ca$ are shown in Fig. 6 for five lab energies. Absolute normalization of the data was accomplished by integrating a smooth curve drawn through each set of data points and setting the sum equal to the absolute total cross section at that energy. At angles less than about 80°, the data coincided with the SCT theory[4–7]; consequently these curves were used as a guide in the integration process in extrapolating to small angles beyond the data. A value of 15% was assigned to the error in the absolute differential-cross-section values.

C. Total Cross Sections

The total cross sections for $^{10}B(^{14}N,^{11}C)^{13}C$ and $^{10}B(^{14}N,^{13}N)^{11}B$ are plotted as a function of energy in Figs. 7 and 8. The energy value associated with each cross-section value is the mean effective energy[1] in the target rather than the energy at the center of the target. This small correction amounted to 0.05-MeV lab for the thinnest target and 0.09 MeV for the thickest.

The error bar associated with each point in Figs. 7 and 8 represents the standard deviation calculated for the initial activity by least-squares analysis, and in addition contains a 5% estimated error due to possible beam fluctuations during bombardment and a 5% error for target thickness. The systematic error (error common to all cross sections) for the boron reactions is assigned a value of 10%. This value is based on a 4%

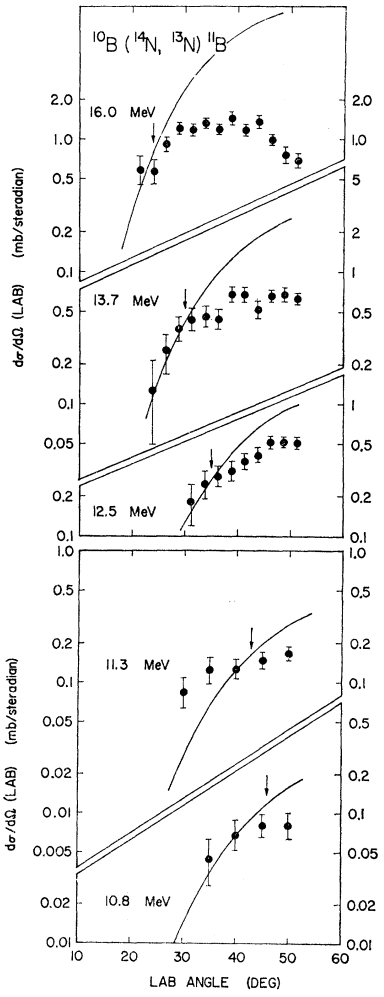

FIG. 5. Angular distributions of ^{13}N from $^{10}B(^{14}N,^{13}N)^{11}B$. SCT theoretical curves shown with the data are normalized to 13.7 MeV, and the arrows predict the onset of nuclear absorption.

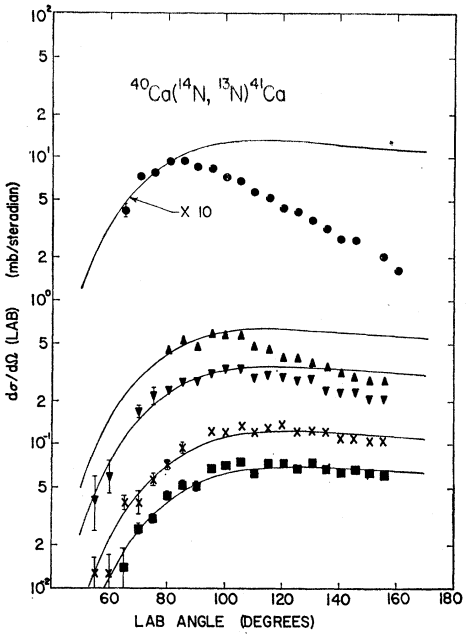

FIG. 6. Angular distributions of ^{13}N from ^{40}Ca(^{14}N,^{13}N)^{40}Ca. Data include transfers to excited states as well as the ground state. The SCT curves are not normalized, but have been drawn independently through each set of data. Laboratory energies are: circle, 29.5 MeV; upward pointed triangle, 28.4 MeV; downward pointed triangle, 27.5 MeV; cross, 26.2 MeV; square, 25.6 MeV.

error in the counter efficiency calibration, a 2% error for the integrator calibration, and an 8% error due to the uncertainty in the absolute energy.

The results of Gaedke, Toth, and Williams,[3] and the earlier results of Reynolds, Scott, and Zucker[17]—both results obtained by "thick-target" methods—are included in Figs. 7 and 8 for comparison. Within the errors, the data of Gaedke *et al.* are in agreement with our data except at the highest energies for the ^{10}B(^{14}N,^{13}N)^{11}B reaction. The data of Reynolds *et al.* appear to be higher in cross section for both reactions.

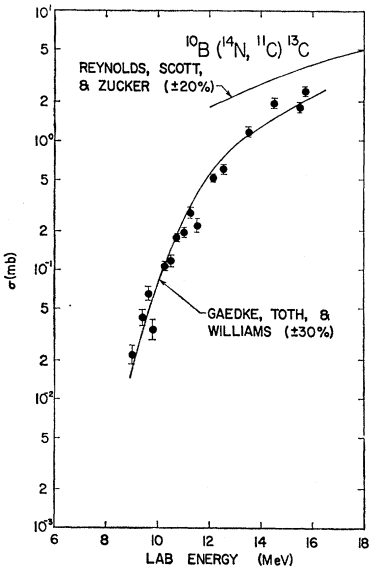

FIG. 7. Total-cross-section data for the ^{10}B(^{14}N,^{11}C)^{13}C reaction. The curves represent the experimental data of earlier workers. A systematic error of 10% common to all points is assigned to the data in addition to the error bars of the individual points.

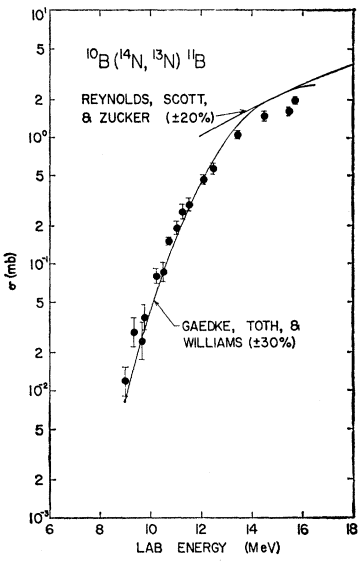

FIG. 8. Total-cross-section data for the ^{10}B(^{14}N,^{13}N)^{11}B reaction. The curves represent the experimental data of earlier workers. A systematic error of 10% common to all points is assigned to the data in addition to the error bars of the individual points.

The results of the total-cross-section measurements for ^{40}Ca(^{14}N,^{13}N)^{41}Ca are plotted in Fig. 9. The cross-

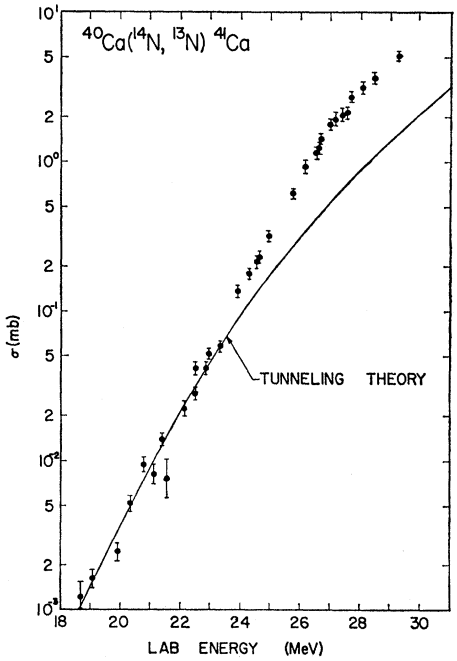

FIG. 9. Total-cross-section data for the ^{40}Ca(^{14}N,^{13}N)^{40}Ca reaction. The SCT theory curve is normalized to the low-energy data. A systematic error of 18% common to all points is assigned to the data in addition to the error bars of the individual points. The data include transfers to both the ground state and excited states of ^{41}Ca. The SCT curve drawn through the low-energy points applies only to transfer between $p_{1/2}$ states.

[17] H. L. Reynolds, D. W. Scott, and A. Zucker, Phys. Rev. **102**, 327 (1956).

section values were calculated from the absolute activity on the back-scatter foils where a correction has been included in each case to account for the ^{13}N scattered to other angles. As in the case of ^{10}B, the cross sections are plotted versus the mean effective energy. The errors were evaluated in the same way, except that an additional error of 15%, introduced in taking into account the particles escaping the back-scatter foils, has been combined with the above 10% systematic error to give an 18% error common to all points for this reaction.

IV. DISCUSSION OF RESULTS

A. ^{10}B(^{14}N,^{11}C)^{13}C

While the DWBA and SCT[2,4–7] for neutron transfer cannot be applied to this reaction, there are some interesting features exhibited in the data that merit further discussion. The angular distributions (Fig. 4) appear to change shape with increasing energy, and at 16.0 MeV there are two definite peaks in the data. The 16.3-MeV range distributions (Fig. 1) show that ^{11}C involving only ground states are scattered to angles of 30° and beyond. The 15° and 20° range data show, in addition, the presence of ^{11}C from reaction where ^{13}C was formed in the first excited state. A separation of states is indicated at 15°, 20°, and 30° in Fig. 4 by G and E for ground-state and excited-state transfers, respectively; the dashed curve represents the excited-state contribution to the total angular distribution (^{13}C excited) and the solid line shows the ground-state contribution (neither nucleus excited). These results can be understood from the standpoint of the semiclassical theory if one assumes that the transfer reaction depends primarily on $R_{\min}$, the distance of closest approach for the classical trajectory:

$$R_{\min}=(a'\bar{a}')^{1/2}[1+\csc(\theta(\text{c.m.})/2)]. \quad (1)$$

Here, θ(c.m.) is taken as the center-of-mass scattering angle, $(a'\bar{a}')^{1/2}=Z_1Z_2e^2/(E\bar{E})^{1/2}$, E is the initial center-of-mass energy, and $\bar{E}=E+Q$ is the energy after the reaction has occurred. The angular distributions of both the ground-state and excited-state reactions were therefore recalculated in terms of $R_{\min}$, where

$$\frac{d\sigma}{dR_{\min}}=\left[\frac{8\pi}{(a'\bar{a}')^{1/2}}\right]\sin^3\left(\frac{\theta(\text{c.m.})}{2}\right)\left(\frac{d\sigma}{d\Omega}\right)_{\text{c.m.}}. \quad (2)$$

The $d\sigma/dR_{\min}$ versus $R_{\min}$ plots (not shown) were found to coincide. In other words, the cross sections for ground-state and excited-state transfer were found to be equal at a given reaction distance $R_{\min}$. Thus, the ^{11}C from excited-state transfers follow a trajectory to a larger c.m. angle than those scattering at the same $R_{\min}$ from ground-state reactions because of their smaller kinetic energy in the final system. This effect leads, therefore, to a smaller lab angle relative to the incident beam for the ^{11}C associated with the excited state of ^{13}C. (Recall that the ^{11}C are the recoil particles in this reaction.)

B. ^{10}B(^{14}N,^{13}N)^{11}B

The range data show no evidence of reactions involving excited states of ^{11}B. If one assumes the same $R_{\min}$ for ground-state and excited-state reactions as in the preceding section, a lab angle of 36° for ^{13}N from excited-state transfer corresponds to θ(lab)=30° (where the cross section is large) for ground-state transfer. Since no ^{13}N from excited-state reactions were detected at either 30° or 40° (Fig. 1), it is concluded that excited-state contributions to the total transfer are not appreciable at 16.3 MeV and, presumably, not at lower energies either.

The SCT theory[4–7] has been compared to the differential-cross-section data in Fig. 5, where the individual theoretical curves have been transformed to the lab system by standard methods.[18] Of the two possible c.m. cross-section values to be transformed to each lab angle, only the value corresponding to the smaller c.m. angle was used since the large-angle ^{13}N do not have sufficient energy to escape the target. The 13.7-MeV curve was fitted to the small-angle data points at that energy, and the other curves were normalized to this 13.7-MeV curve by use of Eqs. (2) and (4.15) of Ref. 7.

The 13.7-MeV data begin to deviate from the theory at angles greater than 30° (lab), which can be interpreted as nuclear absorption occurring within some radius R_a. This same absorption radius was used at the other energies in calculating the angle at which absorption should begin to occur from Eq. (1). These absorption angles are indicated by arrows in Fig. 5.

The data of Fig. 5 tend to be consistent with a picture of tunneling plus close-collision absorption, except possibly for the two small-angle points at 11.3 MeV. Aside from these two points, the tunneling theory fits the data on the small-angle side of the arrows, while it lies above the data on the large-angle, or nuclear-absorption, side of the arrows. The nuclear absorption would presumably disappear when the laboratory energy is reduced below 9.4 MeV.

The cause of the discrepancy between the two points at 11.3 MeV mentioned above is not known. Virtual Coulomb excitation (VCE)[19] is not considered to be a likely cause, because the 10.8-MeV data are in agreement with tunneling (VCE would be expected to be stronger relative to tunneling at this lower energy).

The total-cross-section data are shown in Fig. 10 with the SCT tunneling theory; the theory has been normalized to the low-energy points. The Q value for the reaction has been introduced into the theory by averaging the reaction energies and the neutron binding energies for the initial and final states of the reaction as suggested by Breit.[7] As discussed in the Introduction, the tunneling theories as developed so far are specialized in the total-cross-section calculation to the ^{14}N(^{14}N,^{13}N)-^{15}N reaction; thus the curve in Fig. 10 is for orientation purposes only.

[18] R. D. Evans, *The Atomic Nucleus* (McGraw-Hill Book Company, Inc., New York, 1955), p. 421.
[19] G. Breit and M. E. Ebel, Phys. Rev. **104**, 1030 (1956).

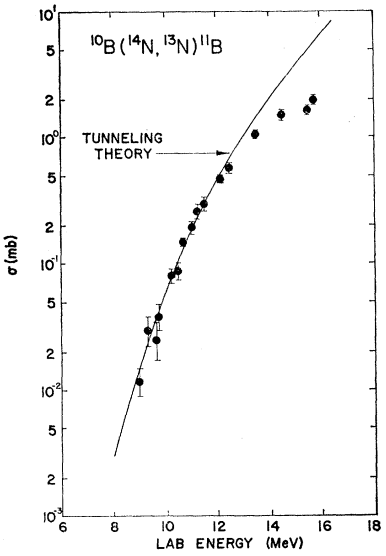

FIG. 10. Total-cross-section data for the ^{10}B(^{14}N,^{13}N)^{11}B reaction plotted with the SCT theoretical curve. Normalization of the curve is made at 9.0 MeV.

C. ^{40}Ca(^{14}N,^{13}N)^{41}Ca

The range data of Fig. 3 show contributions from both ground-state and excited-state transfers. At 29.8 MeV for the 70° data (corresponding to the distant collisions) the ^{13}N from excited states appear significantly. Excited-state transfers contribute strongly at 90° for the 27.5-MeV data, also. These measurements were made in the region where nuclear absorption begins to occur, as seen in the angular-distribution data of Fig. 6; thus the total-cross-section data of Fig. 9 contain ^{13}N from all contributing states.

SCT curves,[4–7] transformed to the lab system, are shown with the data in Fig. 6. A curve has been drawn through the small-angle points of each set of data where tunneling is probably a valid description. No normalization has been made among the various theoretical curves of Fig. 6, as was done for the boron curves (Fig. 5). Comparison of the SCT theory to the data shows good agreement at the lower energies, although the large-angle data may contain contributions from more than one state at even the lowest energies. At the high energies, the data begin to fall below the SCT theory at the largest angles, this being attributed to nuclear absorption occurring within some nuclear radius R_a. An R_a value corresponding to the angles for maximum transfer was calculated from the curves of Fig. 6 and Eq. (1), the average value being $R_a=10.3$ F $\pm 3\%$. A value $r_0=1.78$ F was obtained from the relation $R_a=r_0(A_1^{1/3}+A_2^{1/3})$, where the A_i are the mass numbers of the nuclei involved.

For comparison purposes, a relative SCT curve[4–7] has been fitted to the total-cross-section data of Fig. 9 at the lowest energies where ground-state transfers are most likely to predominate. This curve has been generated, as for the boron case, by averaging the various initial and final parameters in the interaction. From the range data, it is known that transfers to both ground and excited states of ^{41}Ca occur at energies above 27.5 MeV. While no information concerning the ^{41}Ca states is available at lower energies it may be significant that, at energies below the Coulomb barrier, transfers only to the ground state are observed for the ^{14}N(^{14}N,^{13}N)^{15}N and ^{10}B(^{14}N,^{13}N)^{11}B reactions. From the angular-distribution data in Fig. 6 it is seen that nuclear effects disappear below 25.6 MeV, so that this energy may be considered to be the Coulomb barrier in the laboratory system. There is thus a possibility that the transfer process below this energy proceeds only through the ground state of ^{41}Ca.

V. CONCLUSIONS

The data presented here show that the first excited state of ^{13}C as well as the ground state is involved in the transfer of protons in ^{10}B(^{14}N,^{11}C)^{13}C. No transfers involving excited states of ^{11}C were observed. The angular distribution of ^{11}C shows two peaks at an incident energy of 16.0 MeV, which can be understood in terms of the ^{11}C from the ground-state and excited-state transfers being formed at the same minimum interaction distance, but with the ^{11}C from the two states scattering to different angles because of their difference in energy.

The ^{10}B(^{14}N,^{13}N)^{11}B reaction has been shown to involve only ground-state transfers. The angular-distribution data are consistent with the SCT process plus some nuclear absorption. No reduced-width value has been determined from the total-cross-section data because of the inapplicability of the present tunneling calculations to the boron reaction.

Excited-state transfers have been found to be significant in the ^{40}Ca(^{14}N,^{13}N)^{41}Ca reaction, at least at the higher energies ($E>27.5$ MeV); contributions from the ground state and excited states could not be resolved. The angular distributions show good agreement with the SCT process except for the angles which correspond to nuclear absorption occurring at close collisions. Total-cross-section data, which include transfer contributions to several states in ^{41}Ca above 27.5 MeV, have been obtained at energies considerably below the Coulomb-barrier energy of 25.6 MeV. Based on previous experience, these low-energy data may include only transfer processes terminating in the ground state of ^{41}Ca.

Data are therefore available from which neutron reduced-width values can be obtained for ^{11}B and ^{41}Ca. Further calculation with the SCT or DWBA theory is required, however, before such quantities can be determined.

ACKNOWLEDGMENTS

We particularly wish to thank Dr. J. L. Fowler and Dr. A. Zucker for extending to us the hospitality of the Oak Ridge National Laboratory. The helpfulness and support of Dr. C. D. Moak and the accelerator staff are also deeply appreciated. We wish to thank, too, M. R. Cates for his assistance with the experiments. Discussions with Professor G. Breit in connection with the SCT theory are also gratefully acknowledged.